ISSN 2394-3777 (Print)
ISSN 2394-3785 (Online)
Available online at www.ijartet.com
International Journal of Advanced Research Trends in Engineering and Technology (IJARTET)
Vol. 3, Special Issue 2, March 2016

Molecular modeling study on encapsulation of halogenated benzophenones in α- and β-cyclodextrin nanocavities

V. Meenatchi[b], S. Siva[a*] and S. Cholan[c]

[a]Department of Chemistry, Bharathiyar Institute of Engineering for Women Deiyakurichi - 636 112.

[b]Department of Chemistry, Sri Vijay Vidhyalaya College of Arts & Science (Women), Dharmapuri - 636807.

[c]Department of Chemistry, Aringnar Anna College (Arts & Science), Krishnagiri - 635001, Tamil Nadu, India.

* -Corresponding author: sivas7686@yahoo.co.in

Mobile: +91 97880 68821.

ABSTRACT

The geometries of the cyclodextrins (CDs) inclusion complexes with 4-bromobenzophenone (BBP), 4-chlorobenzophenone (CBP) and 4-fluorobenzophenone (FBP) in gas phase were determined by PM3 calculation. Two orientations of the guest were considered: the halogenated benzene ring located near the narrow rim and at the wider rim of the cyclodextrin, respectively. The calculation demonstrates that in all cases the guest molecules are located inside the CD cavity. The preferred complexation orientation is that one, in which the benzene ring 'B' of guest is located near the narrow rim with the primary hydroxyl groups of the CDs. Investigations of thermodynamic and electronic properties confirmed the stability of the inclusion complex. Moreover, the statistical thermodynamic calculations at 1 atm and 298.15 K demonstrate that 1:1 guest/CD complexation is an exothermic process, enthalpically favorable in nature. Non bonded Van der Waals interactions represent the mainly driving forces for the complex stability.

Keywords: BPs, Cyclodextrin, Inclusion complex, Molecular Modeling, Thermodynamic parameters.

1. Introduction

Cyclodextrins (CDs) are well known for their capability to form inclusion complexes with a diverse of molecules, in particular with those having a hydrophobic character [1, 2]. As a consequence of this property, CDs have found substantial interest in supramolecular chemistry [3]. Cyclodextrins are extensively studied cyclic, torus shaped, oligomer of amylose characterized by an inner cavity size and number of glucose units present. These features make CDs capable of hosting molecular guests via inclusion of the whole guest, or part of it, into the void cavity and consequently form supramolecular host–guest complexes [4, 5]. Several forces are known to be accountable for the formation of inclusion complexes of CDs with suitable guest molecules i.e., hydrogen bondings, electrostatic interactions, van der Waals forces, hydrophobic interactions and dipole-dipole interactions [6, 7]. Encapsulation of the guest molecules in the host CDs cavities replicate the physicochemical properties of the guest molecules. For example, bioavailability, solubility, stereo selectivity, catalytic activity, chemical and physical stabilization [8-10].

Parametric method 3 (PM3) has been successfully applied in the study of host-guest interactions with good results [11, 12]. This method has high computational efficiency and its precision is comparable to that of *ab* initio calculations with basis sets at medium level. For large molecular systems such as host-guest inclusion complex, *ab initio* methods are more expensive. PM3 performs better than Austin Method 1 (AM1) in biochemical systems due to its dealing better with hydrogen bonding [13, 14].

2. Molecular modeling

The theoretical calculations were performed with Gaussian 03W package. The initial geometry of the guests, α-CD and β-CD were constructed with the aid of Spartan 08 software and then optimized by Gaussian 03W software package using PM3 method. The CDs were fully optimized by PM3 method without any symmetry constraint [15]. The glycosidic oxygen atoms of CDs were placed onto the XY plane and their centre was defined as the centre of the coordination system. The primary hydroxyl groups were placed pointing

ISSN 2394-3777 (Print)
ISSN 2394-3785 (Online)
Available online at www.ijartet.com
International Journal of Advanced Research Trends in Engineering and Technology (IJARTET)
Vol. 3, Special Issue 2, March 2016

toward the positive Z axis. The inclusion complexes were constructed from the PM3 optimized CDs and guest molecules. The longer dimension of the guest molecule was initially placed onto the Z axis. The position of the guest was determined by the Z coordinate of one selected atom of the guest. The inclusion process was simulated by putting the guest in one end of CD and then letting it pass through the CD cavity.

Two different forms of orientations are considered for the inclusion of guest in to the cavity through the secondary rim of CDs (Fig. 1).

Orientation-A: orientation of benzene ring of 'B' towards the secondary rim of CDs.

Orientation-B: orientation of benzene ring of 'A' towards the secondary rim of CDs.

For the simulation process, the CD was kept in this position while the guest approached along the z-axis toward the wider rim of CD cavity. The orientations of the guest deduced from the results of the investigations in solution were considered. The relative position between guest and CD was calculated by the distance of C_4 atom of the aromatic ring of guest and the secondary rim of host molecule. The guest was initially located at a distance of 6 Å from the cavity rim and then moved in decreasing increments of 2 Å towards the center of the CD cavity. At each step the whole inclusion structure was fully optimized without any constraint using the PM3 method in Gaussian 03W package. So the guest molecule was free to move in the CD cavity during the entire optimization process. Therefore, the conformational changes of the guest and CD molecule were explicitly allowed. In this way, the local minima for the inclusion complex structures were found and further optimized with PM3 method.

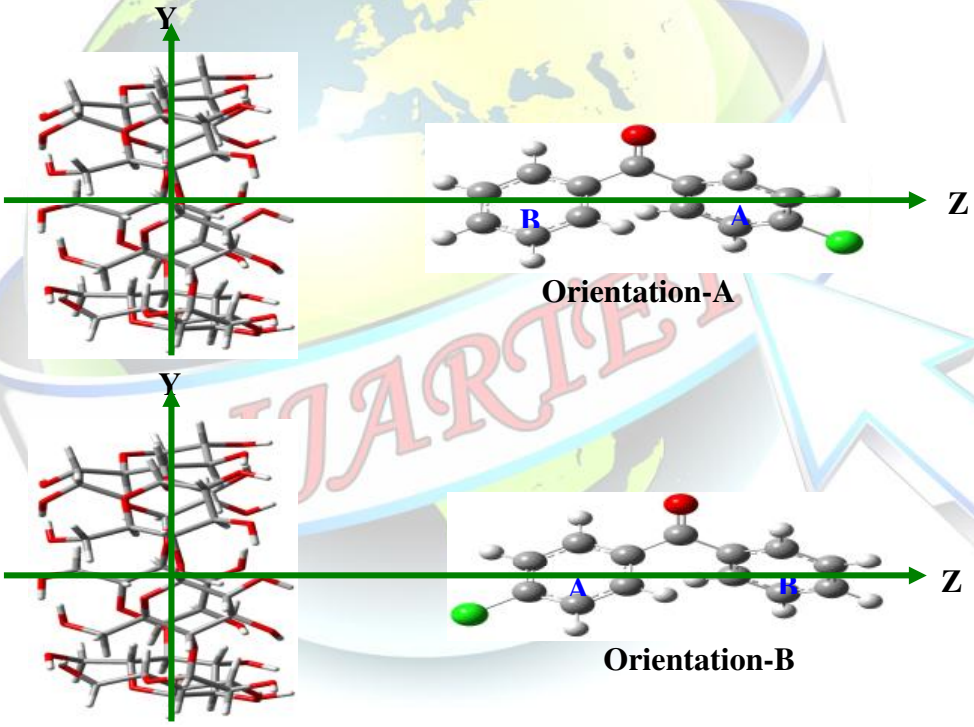

Fig. 1. Coordinate systems to describe inclusion process of CBP with CDs.

Complexation energy upon inclusion complex formations between the guests and the CDs were calculated for the minimum energy structure according to Eqn. (2.1).

$$\Delta E_{complexaton} = E_{complex} - (E_{CD} + E_{guest}) \quad \ldots(2.1)$$

where $E_{complex}$, E_{CD} and E_{guest} represent the total energy of the complex, the free optimized CD and the free optimized guest, respectively.

Enthalpy change upon inclusion complex formations between the guests and the CDs were calculated for the minimum energy structure according to Eqn. (2.2).

$$\Delta H_{complexaton} = H_{complex} - (H_{CD} + H_{guest}) \quad \ldots(2.2)$$

ISSN 2394-3777 (Print)
ISSN 2394-3785 (Online)
Available online at www.ijartet.com
International Journal of Advanced Research Trends in Engineering and Technology (IJARTET)
Vol. 3, Special Issue 2, March 2016

where $H_{complex}$, H_{CD} and H_{guest} represent the total enthalpy of the complex, the free optimized CD and the free optimized guest, respectively.

Gibbs free energy change upon inclusion complex formations between the guests and the CDs were calculated for the minimum energy structure according to Eqn. (2.3).

$$\Delta G_{complexaton} = G_{complex} - (G_{CD} + G_{guest}) \quad \ldots(2.3)$$

where $G_{complex}$, G_{CD} and G_{guest} represent the total free energy of the complex, the free optimized CD and the free optimized guest, respectively.

Entropy change upon inclusion complex formations between the guests and the CDs were calculated for the minimum energy structure according to Eqn. (2.4).

$$\Delta S_{complexaton} = S_{complex} - (S_{CD} + S_{guest}) \quad \ldots(2.4)$$

where $S_{complex}$, S_{CD} and S_{guest} represent the total entropy of the complex, the free optimized CD and the free optimized guest, respectively.

The change in dipole moment upon inclusion complex formations between the guests and the CDs were calculated for the minimum energy structure according to Eqn. (2.5).

$$\Delta D_{complexaton} = D_{complex} - (D_{CD} + D_{guest}) \quad \ldots(2.5)$$

where $D_{complex}$, D_{CD} and D_{guest} represent the total dipole moment of the complex, the free optimized CD and the free optimized guest, respectively.

HOMO as ionization energy (IE) and LUMO as electron affinity (EA) were used for calculating the energy gap, which is calculated by following Eqn. (2.6).

$$Gap = E_{HOMO} - E_{LUMO} \quad \ldots(2.6)$$

The HOMO and LUMO energy were used for calculating the electronic chemical potential (μ), global hardness (η) and softness (S) using the following expressions.

$$\mu = (E_{HOMO} + E_{LUMO})/2 \quad \ldots(2.7)$$

$$\eta = E_{LUMO} - E_{HOMO}/2 \quad \ldots(2.8)$$

$$S = 1/\eta \quad \ldots(2.9)$$

The electrophilicity (ω) of the components are calculated in semiempirical method using the following Eqn. (2.10).

$$\omega = \mu^2/2\eta \quad \ldots(2.10)$$

3. Results and discussion

3.1. Optimization of inclusion complexes

Molecular modeling study (semiempirical quantum mechanical calculation) was carried out to analyse the mode of interaction between three BPs and CDs. This study revealed that a preferred final relative orientation for all the inclusion complexes occurred in spite of the different initial configurations arbitrarily imposed. The molecular structure of all BPs consists of two phenyl moieties and halogen atom (Fig. 2). The phenyl moiety along with carbonyl group of guest molecule insert from the wider rim of the CD cavity, because generally the approach of the guest molecules to the CD cavity is more favorable towards from the wider rim side of the cavity. In addition, when the guest molecule inserted into the wider cavity of CD, the guest may rotate much more freely than that from the narrower rim. The CD molecule has a truncated cone shaped macro ring built of six (α-CD) and seven (β-CD) glucopyranose units. The internal diameter of the α- and β-CD was found to be approximately ~ 5.6 and 6.5 Å, respectively and its height ~7.8 Å. According to the molecular dimensions of BPs (long axis: BBP ≈ 10.0137 Å; CBP ≈ 9.7663 Å; FBP ≈ 9.3521 Å), it is too large to fit entirely in the CDs cavity and the entire guest molecules cannot fully entrapped in the hydrophobic cavity. After optimizing the geometries for the separate molecules, the phenyl ring 'A' or 'B' of guest molecules was placed inside the CD cavity and a fully optimization with frequency analysis on these complexes. Several initial modes of inclusion were probed and optimized by energy minimization. The complex structure leading to the minimum heat of formation shows the phenyl ring along with carbonyl group located at inside of the CD cavity. On the other hand the BPs prefer to include the cavity of CDs from its wide side rather than the narrow side.

ISSN 2394-3777 (Print)
ISSN 2394-3785 (Online)
Available online at www.ijartet.com
International Journal of Advanced Research Trends in Engineering and Technology (IJARTET)
Vol. 3, Special Issue 2, March 2016

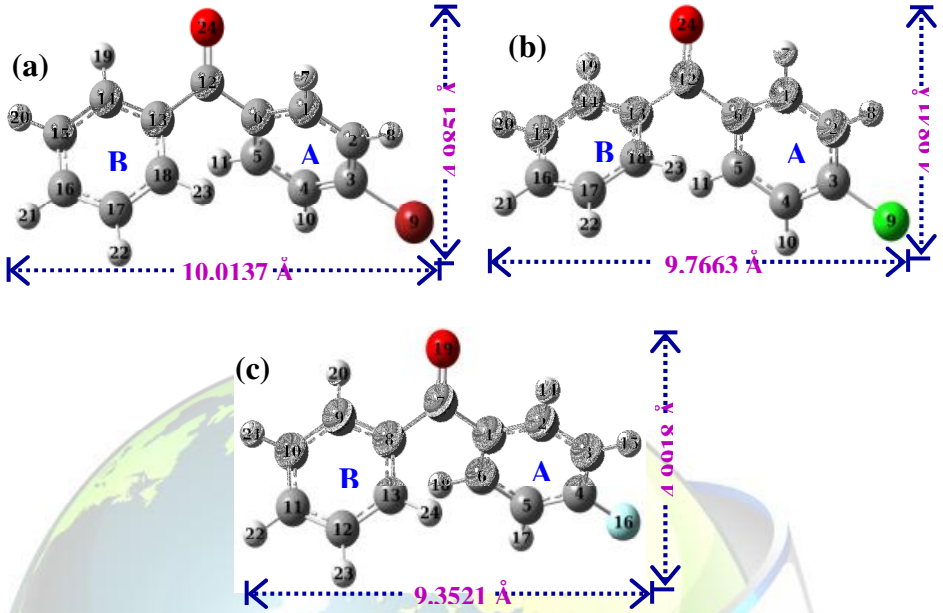

Fig. 2. PM3 optimized ground state structure with numbering system of (a) BBP, (b) CBP and (c) FBP, Colors of the atoms indicates: grey ~ carbon, white ~ hydrogen, red ~ oxygen, brown ~ bromine, green ~ chlorine and sky blue ~ fluorine of the molecules respectively.

Figs. 3-5 display the side view of the most stable inclusion complexes of BBP/CD, CBP/CD and FBP/CD respectively. In Tables 3.1 and 3.2, we listed the energies, HOMO, LUMO and dipole moment values for the free guest and the inclusion complexes obtained from PM3 method. In all the structures, a considerable part of the guest molecule is accommodated into the CD cavity. The long axis of the guest is oriented along the axis of the CD, with the phenyl ring positioning within the cavity. The minimum energy structure also revealed that the guests are included along the molecular axis of CD, but its molecular axis is not exactly perpendicular to the CD symmetry axis, rather it is slightly tilted to allow maximum hydrogen bonding between the host and the guest molecules. In all the three cases, the preferred orientation for complex formation is that one, in which the benzene ring of guest is located near the wider rim comprising the secondary hydroxyl groups.

ISSN 2394-3777 (Print)
ISSN 2394-3785 (Online)
Available online at www.ijartet.com
International Journal of Advanced Research Trends in Engineering and Technology (IJARTET)
Vol. 3, Special Issue 2, March 2016

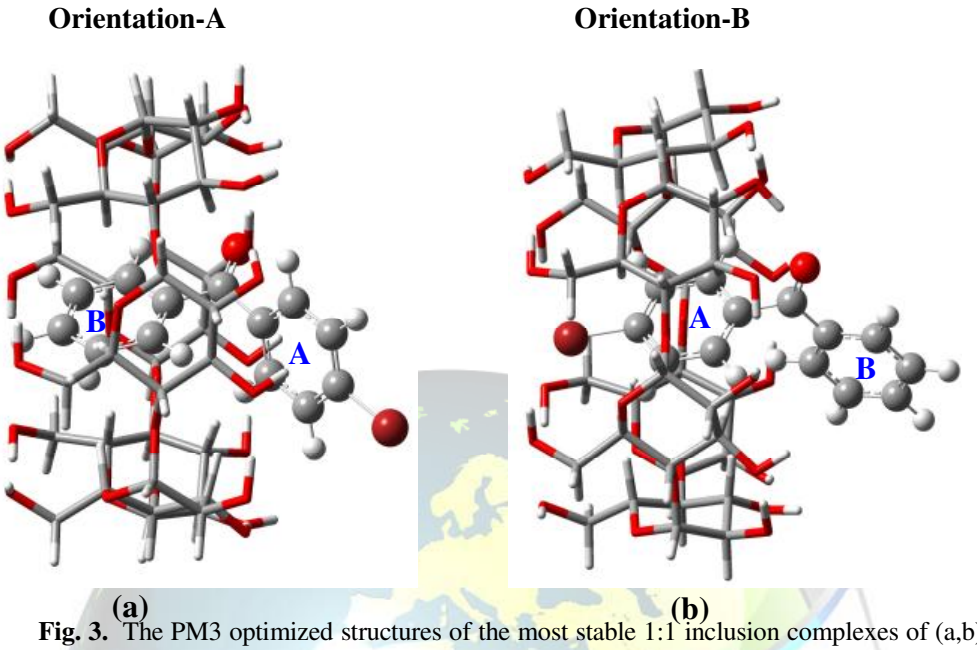

Fig. 3. The PM3 optimized structures of the most stable 1:1 inclusion complexes of (a,b) BBP/α-CD and (c,d) BBP/β-CD in both orientations (A and B).

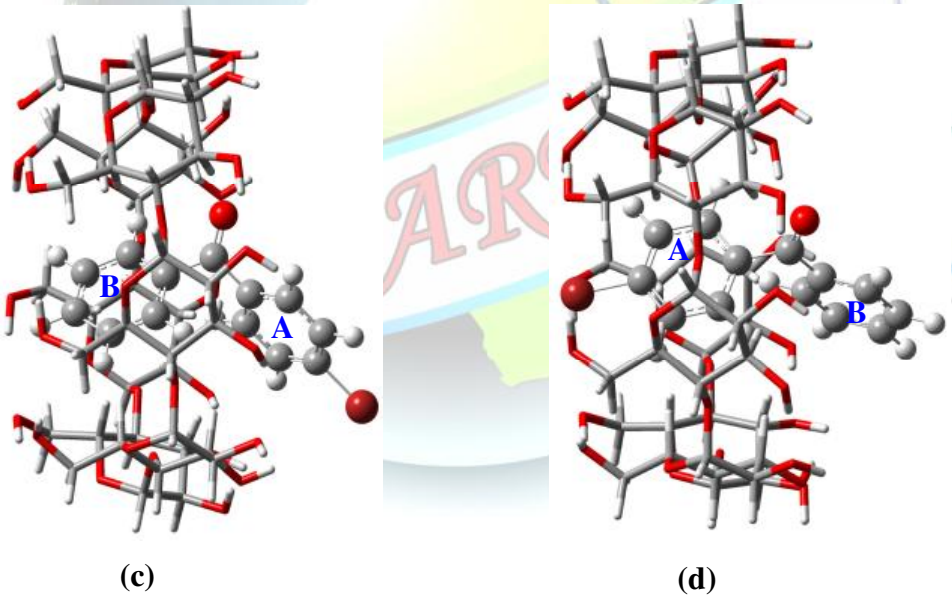

ISSN 2394-3777 (Print)
ISSN 2394-3785 (Online)
Available online at www.ijartet.com
International Journal of Advanced Research Trends in Engineering and Technology (IJARTET)
Vol. 3, Special Issue 2, March 2016

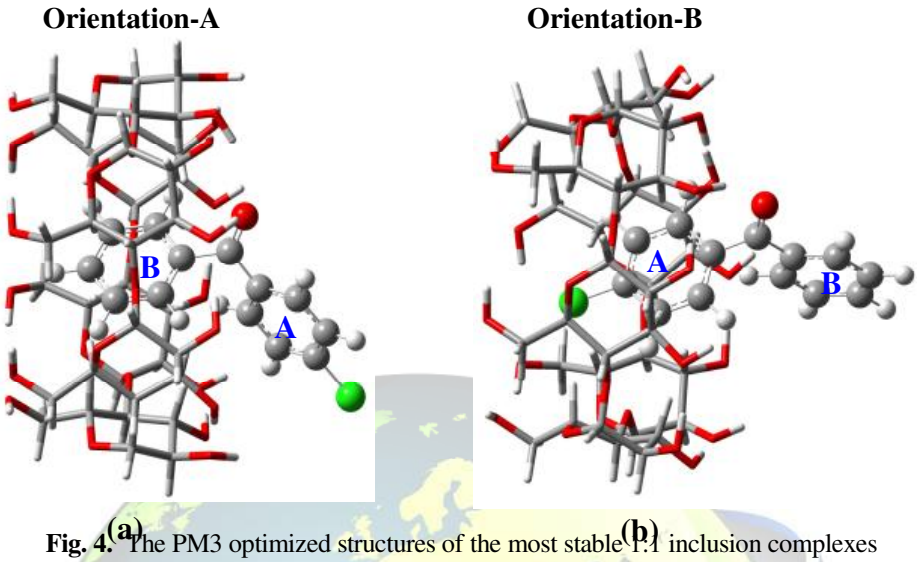

Fig. 4. The PM3 optimized structures of the most stable 1:1 inclusion complexes of (a,b) CBP/α-CD and (c,d) CBP/β-CD in both orientations (A and B).

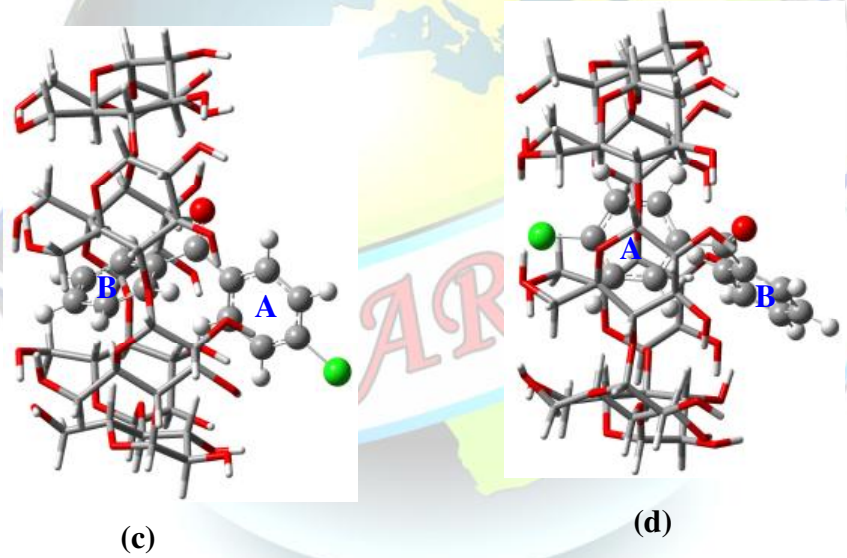

ISSN 2394-3777 (Print)
ISSN 2394-3785 (Online)
Available online at www.ijartet.com
International Journal of Advanced Research Trends in Engineering and Technology (IJARTET)
Vol. 3, Special Issue 2, March 2016

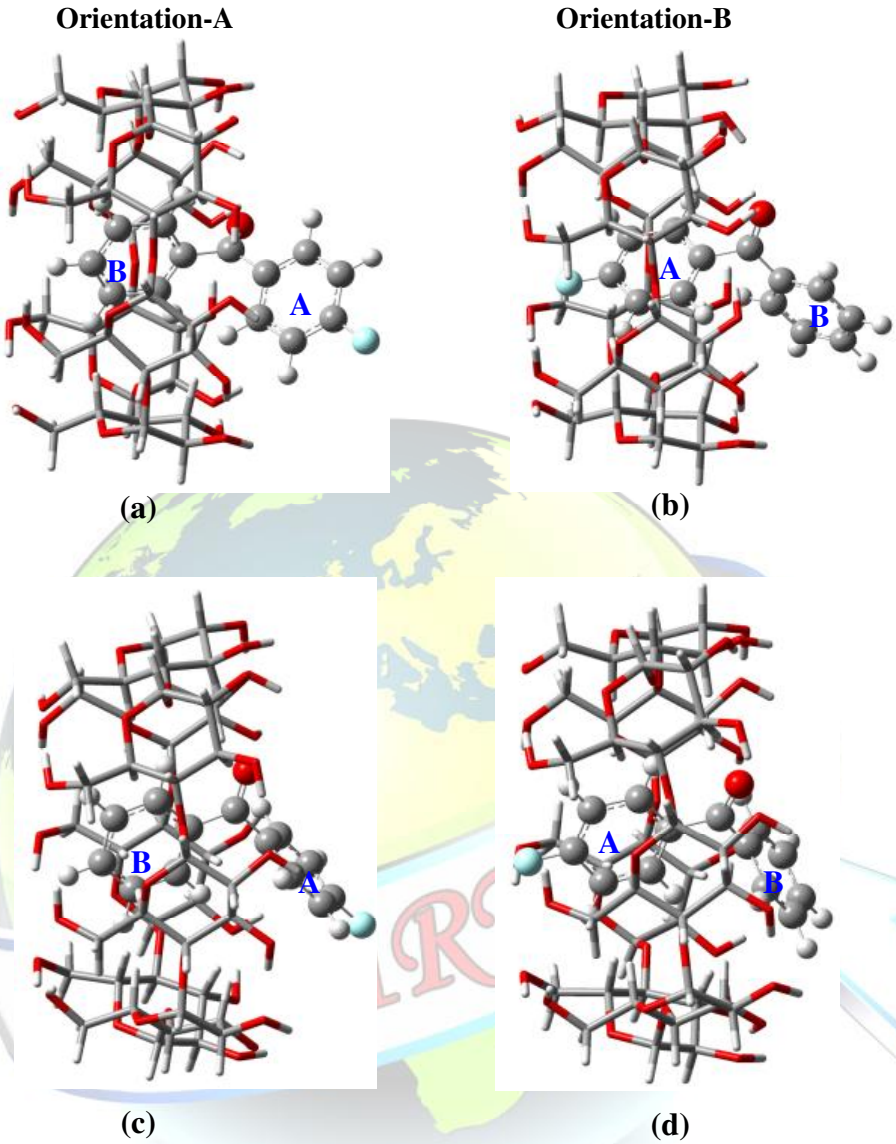

Fig. 5. The PM3 optimized structures of the most stable 1:1 inclusion complexes of (a,b) FBP/α-CD and (c,d) FBP/β-CD in both orientations (A and B).

ISSN 2394-3777 (Print)
ISSN 2394-3785 (Online)
Available online at www.ijartet.com
International Journal of Advanced Research Trends in Engineering and Technology (IJARTET)
Vol. 3, Special Issue 2, March 2016

Table 1. Energetic features, thermodynamic parameters and HOMO-LUMO energy calculations for CBP, α-CD, β-CD and the 1:1 inclusion complexes by PM3 method.

Properties	BBP	α-CD	β-CD	BBP/α-CD		BBP/β-CD	
				Orien-A	Orien-B	Orien-A	Orien-B
E_{HF} (kcal.mol^{-1})	25.09	-1247.62	-1457.75	-1250.19	-1248.38	-1472.69	-1468.98
ΔE (kcal.mol^{-1})				-27.66	-25.85	-40.03	-36.32
H (kcal.mol^{-1})	145.96	-570.84	-667.55	-431.23	-429.97	-530.22	-526.90
ΔH (kcal.mol^{-1})				-6.36	-5.09	-8.63	-5.31
G (kcal.mol^{-1})	112.39	-676.37	-789.52	-551.88	-554.31	-673.87	-672.73
ΔG (kcal.mol^{-1})				12.10	9.67	3.26	4.40
S (kcal/mol-Kelvin)	0.112	0.353	0.409	0.408	0.412	0.481	0.489
ΔS (kcal/mol-Kelvin)				-0.057	-0.053	-0.040	-0.032
E_{HOMO} (eV)	-9.97	-10.37	-10.35	-9.83	-9.77	-9.72	-9.60
E_{LUMO} (eV)	-0.57	1.26	1.23	-0.67	-0.62	-0.51	-0.60
$E_{HOMO-LUMO}$ (eV)	-9.41	-11.63	-11.58	-9.16	-9.15	-9.21	-8.99
Dipole moment (D)	2.52	11.34	12.29	7.71	8.34	11.00	12.72
ΔD				-6.15	-5.52	-3.81	-2.09
μ	-5.27	-4.55	-4.56	-5.25	-5.19	-5.11	-5.10
η	4.70	5.81	5.79	4.58	4.58	4.60	4.50
S	0.21	0.17	0.17	0.22	0.22	0.22	0.22
ω	2.95	1.78	1.79	3.01	2.95	2.84	2.89
$ZPVE^{e}$ (kcal.mol^{-1})	112.86	635.08	740.57	750.01	749.95	854.38	853.67

ISSN 2394-3777 (Print)
ISSN 2394-3785 (Online)
Available online at www.ijartet.com

tional Journal of Advanced Research Trends in Engineering and Technology (IJARTET)
Special Issue 2, March 2016

Table 2. Energetic features, thermodynamic parameters and HOMO-LUMO energy calculations for CBP, FBP and the 1:1 inclusion complexes by PM3 method.

Properties	CBP	CBP/α-CD		CBP/β-CD		FBP	FBP/α-CD		FBP/β-CD	
		Orien-A	Orien-B	Orien-A	Orien-B		Orien-A	Orien-B	Orien-A	Orien-B
E_{HF} (kcal.mol^{-1})	10.55	-1250.24	-1249.03	-1463.65	-1460.96	-26.34	-1285.13	-1284.59	-1497.89	-1494.38
ΔE (kcal.mol^{-1})		-13.17	-11.96	-16.45	-13.76		-11.17	-10.63	-13.80	-11.29
H (kcal.mol^{-1})	132.08	-449.84	-448.86	-544.16	-543.37	96.45	-483.26	-483.16	-578.58	-578.40
ΔH (kcal.mol^{-1})		-11.08	-10.10	-8.69	-7.90		-8.87	-8.77	-7.48	-7.30
G (kcal.mol^{-1})	96.42	-570.93	-572.15	-686.77	-685.81	61.83	-602.50	-603.85	-721.46	-720.49
ΔG (kcal.mol^{-1})		9.01	7.80	6.33	7.28		12.05	10.70	6.24	7.20
S (kcal/mol-Kelvin)	0.119	0.406	0.413	0.477	0.478	0.116	0.400	0.404	0.476	0.479
ΔS (kcal/mol-Kelvin)		-0.066	-0.059	-0.051	-0.050		-0.069	-0.065	-0.049	-0.046
E_{HOMO} (eV)	-9.59	-9.73	-9.58	-9.72	-9.13	-10.00	-9.98	-9.99	-9.81	-9.69
E_{LUMO} (eV)	-0.59	-0.84	-0.91	-0.64	-0.68	-0.64	-0.89	-0.80	-0.60	-0.52
$E_{HOMO-LUMO}$ (eV)	-9.00	-8.89	-8.67	-9.08	-8.45	-9.36	-9.09	-9.19	-9.20	-9.17
Dipole moment (D)	2.49	6.89	8.52	12.76	13.11	2.42	6.93	8.20	11.00	13.99
ΔD		-6.94	-5.31	-2.02	-1.67		-6.83	-5.56	-3.71	-0.72
μ	-5.09	-5.28	-5.25	-5.18	-4.90	-5.32	-5.43	-5.40	-5.20	-5.10
η	4.50	4.44	4.33	4.54	4.22	4.68	4.54	4.60	4.60	4.58
S	0.22	0.22	0.23	0.22	0.24	0.21	0.22	0.22	0.22	0.22
ω	2.87	3.14	3.17	2.95	2.85	3.03	3.25	3.17	2.94	2.84
ZPVE (kcal.mol^{-1})	113.10	750.69	750.00	854.69	854.53	114.65	752.05	752.39	855.91	856.49

ISSN 2394-3777 (Print)
ISSN 2394-3785 (Online)
Available online at www.ijartet.com
International Journal of Advanced Research Trends in Engineering and Technology (IJARTET)
Vol. 3, Special Issue 2, March 2016

The complexation energies of the guest molecules with α-CD and β-CD obtained from the PM3 calculations are given in Tables 1 and 2. The PM3 results showed that the complexation energies (in kcal mol^{-1}) of all the complexes (BBP/α-CD ≈ orien-A = -1250.19, orien-B = -1248.38; BBP/β-CD ≈ orien-A = -1472.69, orien-B = -1468.98; CBP/α-CD ≈ orien-A = -1250.24, orien-B = -1249.03; CBP/β-CD ≈ orien-A = -1459.65, orien-B = -1458.96; FBP/α-CD ≈ orien-A = -1285.13, orien-B = -1284.59; FBP/β-CD ≈ orien-A = -1492.89, orien-B = -1491.38) are negative which demonstrates the inclusion process is thermodynamically favour for both orientations (A and B). Further, the more negative is the complexation energy obtained the more stable is the complex and the more favourable is the configuration. It was found that the complexation energy for orientation-A in each step was always lower than that of orientation-B. These results revealed that the complexation energy is in more favour for the orientation-A with small energy gap and the nature of the driving forces leading to the favourable orientation. Hence, the most stable structures were gathered from the energies of the complexes for probable orientations in which the phenyl ring 'B' located within the CD cavity.

3.2. Thermodynamics of inclusion process

To investigate the thermodynamics of the binding process, the binding energies (ΔE), enthalpy changes (ΔH), Gibbs free energy changes (ΔG) and entropy changes (ΔS), we carried out the statistical thermodynamic calculations for orientation-A at 1 atm pressure and 298.15 K temperature. The thermodynamic parameters are summarized in Tables 1 and 2. The binding energy (ΔE) can be used to evaluate the inclusion process and to find the most stable inclusion complex among the studied complexes. To inspect the stability of the respective inclusion complexes, the binding energy was obtained from the difference between the energy of the inclusion complex and the sum of total energy of the isolated guest and CD molecules. These data provide quantitative measures of the interaction forces driving the complexation process. Once again the large negative binding energy (ΔE) for the formation of complexes in orientation-A revealed that the CDs could form stable complexes with BPs. However, the difference of binding energies for the inclusion complexes of the guests with CDs is 12.37 kcal mol^{-1} (for BBP), 0.72 kcal mol^{-1} (for CBP) and 2.37 kcal mol^{-1} (for FBP) respectively. The binding energies (ΔE) suggest that BPs are highly miscible with both CDs. Further the change in the magnitude of the ΔE would be a sign of the driving force towards complexation. The more negative ΔE value suggests that the complex is more thermodynamically favorable in nature [16]. From the view point of energy, it could be concluded that the binding energies of BBP/CD complexes were 14.49-46.49 kcal mol^{-1} (for α-CD) and 27.58-31.23 kcal mol^{-1} (for β-CD) lower than that of other guest/CD complexes. The calculated binding energies of the inclusion complexes were in sequence of BBP/β-CD < BBP/α-CD < CBP/α-CD < CBP/β-CD < FBP/α-CD < FBP/β-CD. The above sequence revealed that the BBP formed more stable inclusion complexes with β-CD in comparison to that of other CD complexes. Moreover, the difference in the magnitude of the energetic contribution of van der Waals interaction and the complexation energy is an indication of the driving forces responsible for the stability of the BPs/CD complexes.

In all the cases, the β-CD inclusion complexes have larger binding energies when compared to α-CD complexes (Tables 1 and 2). The larger negative binding energy of β-CD complexes indicates that more stable inclusion complexes are formed between the guests and β-CD. This may explain why the addition of β-CD offers better solublization of the above guest molecules than α-CD. It can also be seen from Figs. 3-5, the guest fits more deeply in the cavity of β-CD. However, this behavior is not demonstrated by the guest/α-CD complex.

Engeldinger et al. have reported that the α-CD cavity presents chlorophillic characteristics to the chlorides of transition metals [17–19]. These authors report a weak interaction between the chlorine atom and the H_5 of α-CD with a distance of 2.64 Å. Matias et al. have also presented a Cl-H_3 interaction with a minimum distance of 2.87 Å in 2-chloro benzophenone-β-CD complex [20]. These results indicate that the CD also has some affinity for chlorine. In contrast for CBP/CD complexes, the chlorine atom is not present inside of the CD cavity, suggest that the position of substitution may play an important role in the inclusion complexation process.

The complexation reactions of all BPs with both CD are exothermic judged from the negative enthalpy changes. And the negative ΔH values suggest that all the inclusion processes are enthalpically favorable in nature. Additionally, it can also be seen in Tables 1 and 2 that ΔS values are also negative, this indicates that the formation of the inclusion complex becomes an enthalpy-driven process. Hence these inclusion processes are enthalpy driven process. It should be noted that ΔH and ΔS values were contributions

ISSN 2394-3777 (Print)
ISSN 2394-3785 (Online)
Available online at www.ijartet.com
International Journal of Advanced Research Trends in Engineering and Technology (IJARTET)
Vol. 3, Special Issue 2, March 2016

from (i) release of water molecules from the CD cavity, (ii) partial destruction of hydration shells of the reagents, (iii) non covalent interactions like van der Waals, hydrophobic and hydrogen bonding and (iv) hydration of the inclusion complexes. All the above process should be taken into account while discussing thermodynamic parameters of complex formation. It has been reported that the entropy of complexation depends on the insertion of the drug molecules and the concurrent displacement of water molecules that are trapped within the CD cavity. Experimental results from X-ray [21] and neutron diffraction [15] as well as theoretical studies [22] have indicated that there are seven water molecules, on an average within the CD cavity when it is in aqueous medium.

The enthalpy change for the CBP/α-CD inclusion complex was more negative (–11.08 kcal mol^{-1}) than that of other inclusion complexes, which is certainly attributed to more tightly van der Waals interactions between CD and guest [16, 23]. Thus, we can conclude that the effect of methyl groups upon the complexation is too strengthening the van der Waals interactions. The negative enthalpy changes together with the negative entropy changes suggest that all the inclusion processes are enthalpy driven in nature.

In the literature, The theoretical free energy change (ΔG) values for the inclusion complexes were different from the experimental findings. This can be explained by the solvent effect. The actual experiments are conducted in aqueous medium but the computational work was done at vacuum phase. Unfortunately, because of limitations in the calculation ability of our computer and the large molecular size of CD, the theorietical calculations for these insclusion systems could not be performed for aqueous solutions as well as in excited state. However, it was observed that the solvent effect on the host-guest interactions easily changes the inclusion reaction from a nonspontaneous process in the gas phase to a spontaneous one in the aqueous phase. Further, the host-guest interaction causes an enthaply-entropy compensating process in the gas phase, whereas the same interaction causes an enthalpy-entropy codriven process in aqueous solution, because inclusion complexation releases a number of water molecules from the cavity of CD.

In addition from PM3 calculations, we also noticed that the dipole moment values of free BPs increase when the guest enters into the CD cavity. Further the variation in the dipole moment of different complexes indicates a strong correlation of the polarity with the inclusion process.

3.3. Geometrical parameters

Further studies on the geometrical structures of the inclusion complexes were also made in order to explore the stability of these complexes. From Fig. 6, it can be seen that the guests are almost encapsulated in the cavity of CD molecules. In addition, there are several intermolecular H-bondings present in the complex structures. Here, the H-bondings are defined as C–H···O or C–O···H with the distance $d_{H\cdots O}$ or $d_{O\cdots H}$ less than 3.0 Å [23]. These findings indicated that intermolecular H-bonds played a crucial role in the stability of these inclusion complexes. Considering the shape and dimensions of the host, the guests may not be completely embedded into the CD cavity. Since the vertical distance and length of the guests were greater than the dimensions of the host, the guest molecules cannot be completely accommodated within the CD cavity. Further, the optimized theoretical structures of the guest/CD inclusion complex also confirm that the guest molecules were partially included in the CD cavity. Obviously the H-bondings of β-CD complex are more than that of α-CD complex. This explains why the binding energy of the inclusion complexes of β-CD is noticeably lower than that of α-CD complexes. Further, van der Waals interactions between the guest and host molecules are the most important contribution to the stabilization of these complexes in vacuum. These effect leads to a decrease in the freedom of rotation of complexed molecules giving rise to more ordered system [24-26].

The geometrical parameters namely bond distance, bond angle and dihedral angle of the above guest molecules before and after complexation in α-CD and β-CD obtained from the PM3 optimized most stable structures are presented in Tables 3-5. The calculated parameters evidently showed that the geometry of the guest is distorted. It was also found that a great distortion in dihedral angles when compared to other parameters. This indicates that the drugs adopt a specific conformation to form stable inclusion complex. However, the CD cavity also distorted to a greater extent upon complexation. Further the PM3 results revealed that non-bonded interaction played an important role in the stability of the guest/CD complex, which was also essential for the complex formation.

ISSN 2394-3777 (Print)
ISSN 2394-3785 (Online)
Available online at www.ijartet.com
International Journal of Advanced Research Trends in Engineering and Technology (IJARTET)
Vol. 3, Special Issue 2, March 2016

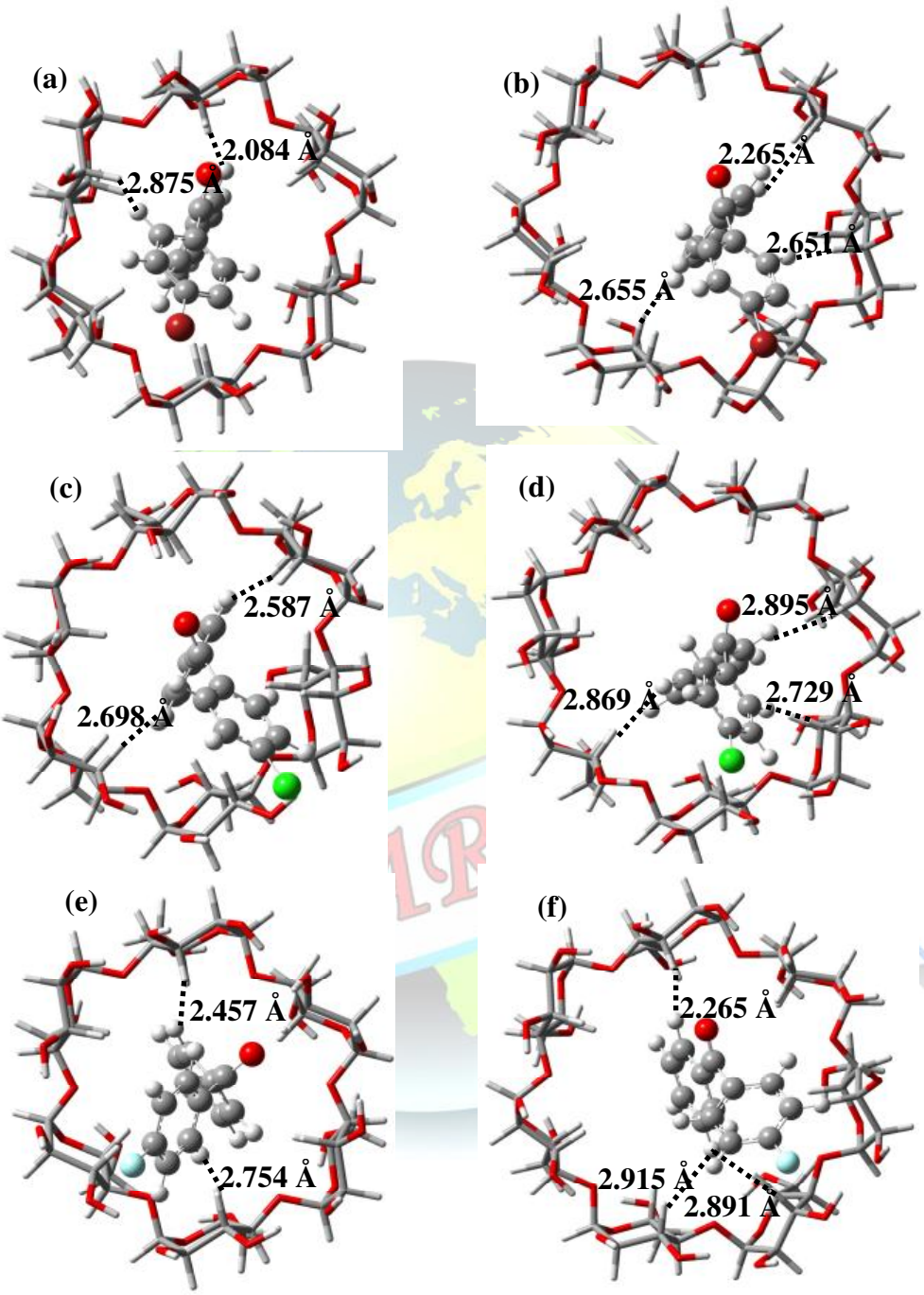

Fig. 6. Upper view of the PM3 optimized structures of the most stable 1:1 inclusion complexes of (a) BBP/α-CD, (b) BBP/β-CD, (c) CBP/α-CD, (d) CBP/β-CD, (e) FBP/α-CD and (f) FBP/β-CD in orientation-A.

ISSN 2394-3777 (Print)
ISSN 2394-3785 (Online)
Available online at www.ijartet.com
International Journal of Advanced Research Trends in Engineering and Technology (IJARTET)
Vol. 3, Special Issue 2, March 2016

Table 3. The significant geometrical parameters of BBP before and after inclusion in α-CD and β-CD (orientation-A), bond distances (Å), angle (°) and dihedral angles (°) calculated by PM3 methods.

Parameters	Free BBP	BBP/α-CD	BBP/β-CD
bond lengths (Å)			
C_{12}-O_{24}	1.215	1.221	1.227
C_1-C_{12}	1.495	1.502	1.505
C_1-C_2	1.396	1.402	1.401
C_2-H_7	1.095	1.086	1.098
C_4-Br_9	1.867	1.870	1.871
C_{13}-C_{14}	1.395	1.399	1.398
bond angles (°)			
C_{13}-C_{14}-H_{19}	119.90	120.10	120.65
C_{13}-C_{12}-O_{24}	122.09	121.50	123.01
O_{24}-C_{12}-C_1	121.32	119.45	122.35
C_{12}-C_1-C_2	119.79	120.01	119.99
dihedral angle (°)			
O_{24}-C_{12}-C_1-C_2	56.66	65.47	53.20
C_{12}-C_1-C_2-H_7	0.22	2.10	-1.10
C_{14}-C_{13}-C_{12}-O_{24}	37.46	15.21	52.62
C_{12}-C_{13}-C_{14}-H_{19}	0.27	-3.42	-0.55
H_8-C_3-C_4-Br_9	0.22	-0.62	0.97

Table 4. The significant geometrical parameters of CBP before and after inclusion in α-CD and β-CD (orientation-A), bond distances (Å), angle (°) and dihedral angles (°) calculated by PM3 methods.

Parameters	Free CBP	CBP/α-CD	CBP/β-CD
bond lengths (Å)			
C_{14}-H_{19}	1.096	1.106	1.103
C_{13}-C_{14}	1.395	1.394	1.399
C_{12}-C_{13}	1.492	1.489	1.495

ISSN 2394-3777 (Print)
ISSN 2394-3785 (Online)
Available online at www.ijartet.com
International Journal of Advanced Research Trends in Engineering and Technology (IJARTET)
Vol. 3, Special Issue 2, March 2016

C_{12}-C_6	1.493	1.489	1.498
C_3-Cl_{19}	1.396	1.682	1.688
bond angles (°)			
C_6-C_{12}-C_{13}	116.69	117.55	115.93
C_{13}-C_{12}-O_{24}	121.74	120.16	122.61
O_{24}-C_{12}-C_6	121.55	120.27	123.45
C_2-C_3-Cl_9	119.56	120.61	120.59
dihedral angle (°)			
O_{24}-C_{12}-C_{13}-C_{14}	45.68	53.74	58.84
C_1-C_6-C_{12}-O_{24}	44.69	38.05	47.63
H_8-C_2-C_3-Cl_9	0.15	-0.40	0.47

Table 5. The significant geometrical parameters of FBP before and after inclusion in α-CD and β-CD (orientation-A), bond distances (Å), angle (°) and dihedral angles (°) calculated by PM3 methods.

Parameters	**Free FBP**	**FBP/α-CD**	**FBP/β-CD**
bond lengths (Å)			
C_9-H_{20}	1.121	1.124	1.124
C_1-C_2	1.392	1.393	1.397
C_7-C_8	1.475	1.476	1.464
C_7-C_1	1.445	1.445	1.458
C_4-F_{16}	1.396	1.482	1.488
bond angles (°)			
C_9-C_8-C_7	116.69	118.55	118.93
C_8-C_7-O_{19}	121.74	114.16	115.61
O_{19}-C_7-C_1	124.55	118.27	119.45
C_3-C_4-F_{16}	119.56	121.61	121.59
dihedral angle (°)			
O_{19}-C_7-C_1-C_2	55.68	48.74	49.84
C_9-C_8-C_7-O_{19}	45.63	40.05	48.63
H_{15}-C_3-C_4-F_{16}	0.42	-0.47	0.54

3.4. HOMO and LUMO analysis

Molecular descriptors that are commonly used for elucidating the chemical properties of molecules in terms of its stability and reactivity [27] included the energy of the highest occupied molecular orbital (HOMO),

ISSN 2394-3777 (Print)
ISSN 2394-3785 (Online)
Available online at www.ijartet.com
International Journal of Advanced Research Trends in Engineering and Technology (IJARTET)
Vol. 3, Special Issue 2, March 2016

the energy of the lowest unoccupied molecular orbital (LUMO), and the energy difference of HOMO and LUMO which is also known as energy gap (E_{HOMO}–E_{LUMO}). The former represents the electron-donating ability while the latter represents the electron-withdrawing ability of the molecules. The electronic distribution of the excited state can be qualitatively predicted by examining changes in HOMO or LUMO coefficients since the simplest picture of an electronically excited state can be visualized as being obtained by promotion of an electron from HOMO to LUMO. As sketched in Figs. 5-8, the electronic density in HOMO is mainly localized on the phenyl ring and halogen atom and in LUMO is accumulated on C–C bond of the phenyl ring. Based on the above simple argument one would predict that for all the guets, the most of the charge migration from halogen substituted benzene ring. The PM3 calculations revealed that as the aliphatic chain length increases, both HOMO and LUMO energy level boosted significantly except for FBP where the energy level is slightly dropped as well as the energy gap also decreased (Tables 1 and 2). Furthermore, the energy differences between HOMO and LUMO level represent the stability and chemical reactivity of a molecule; i.e., larger value indicates high molecular stability and low chemical reactivity while small value gives rise to low molecular stability and high chemical reactivity. Therefore, the E_{HOMO}–E_{LUMO} gap can be used as a relative index for the degree of interaction strength between templates and monomers in which lower values indicate higher strengths of interaction. The energy gap of BBP/β-CD or FBP/β-CD is more than those of other complexes. Consequently, β-CD formed more favorable complexes with the guest molecules in comparison to that of α-CD by the energy gap values, which are in good agreement with the calculated results of energy.

For the most stable complex, the physical parameters such as electronic chemical potential (μ), hardness (η), softness (S) and electrophilicity (ω) values are determined from HOMO and LUMO energy of the systems respectively. S has been known as an indicator of overall stability of a chemical system. On comparing μ values of complexes in Tables 1 and 2, remarkable changes were observed from the isolated guest and host molecules. The guest molecules have higher μ value than that of CDs; therefore the guest molecules are expected to act as electron donor in the inclusion complexation. In the case of both η and S values, significant differences are observed when compared with the isolated host molecules but lies within the range that of the guest one.

ISSN 2394-3777 (Print)
ISSN 2394-3785 (Online)
Available online at www.ijartet.com
International Journal of Advanced Research Trends in Engineering and Technology (IJARTET)
Vol. 3, Special Issue 2, March 2016

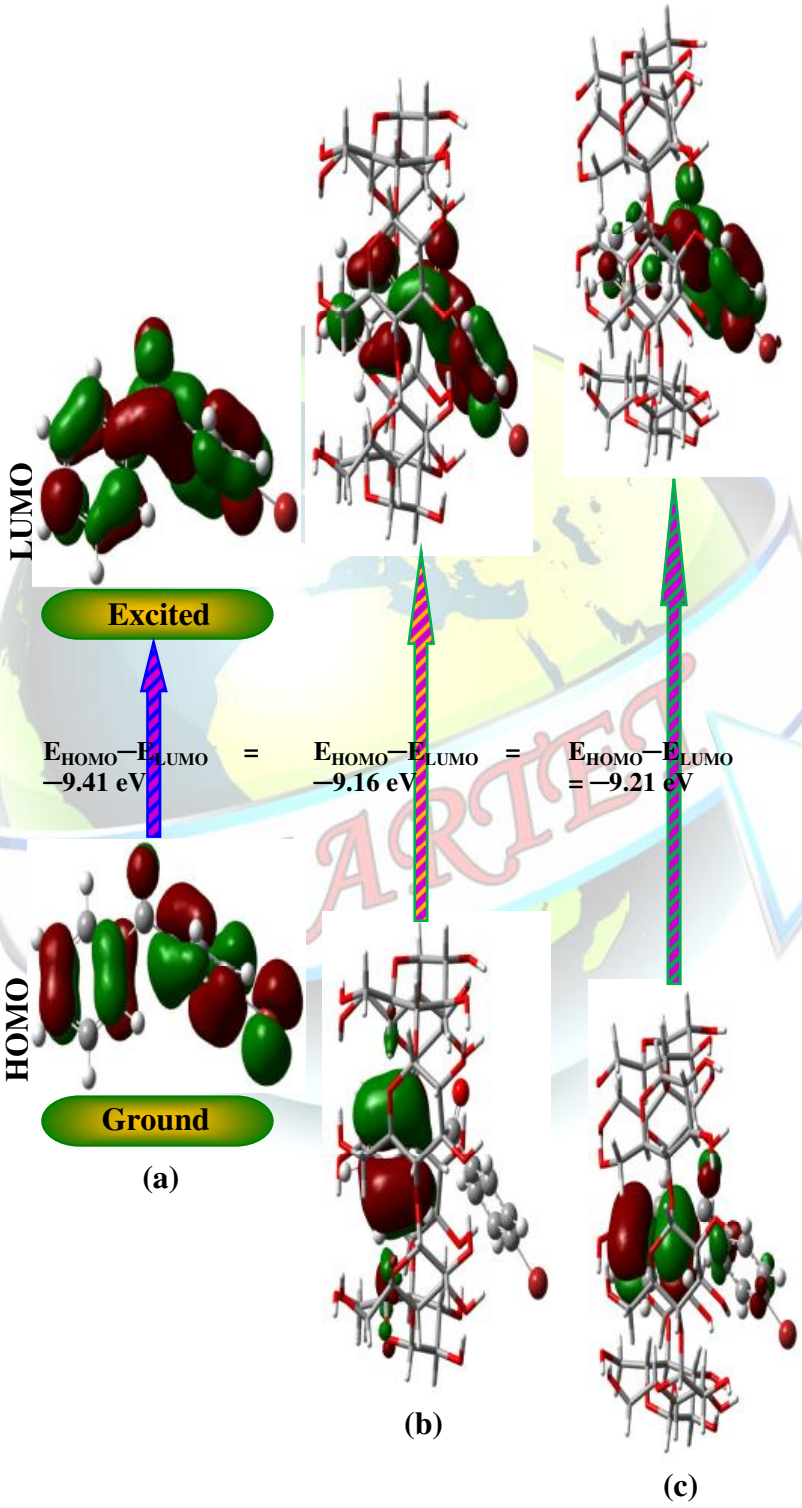

ISSN 2394-3777 (Print)
ISSN 2394-3785 (Online)
Available online at www.ijartet.com
International Journal of Advanced Research Trends in Engineering and Technology (IJARTET)
Vol. 3, Special Issue 2, March 2016

Fig. 6. The atomic orbital compositions of the frontier molecular orbital for (a) BBP, (b) BBP/α-CD (orientation-A) and (c) BBP/β-CD complex (orientation-A).

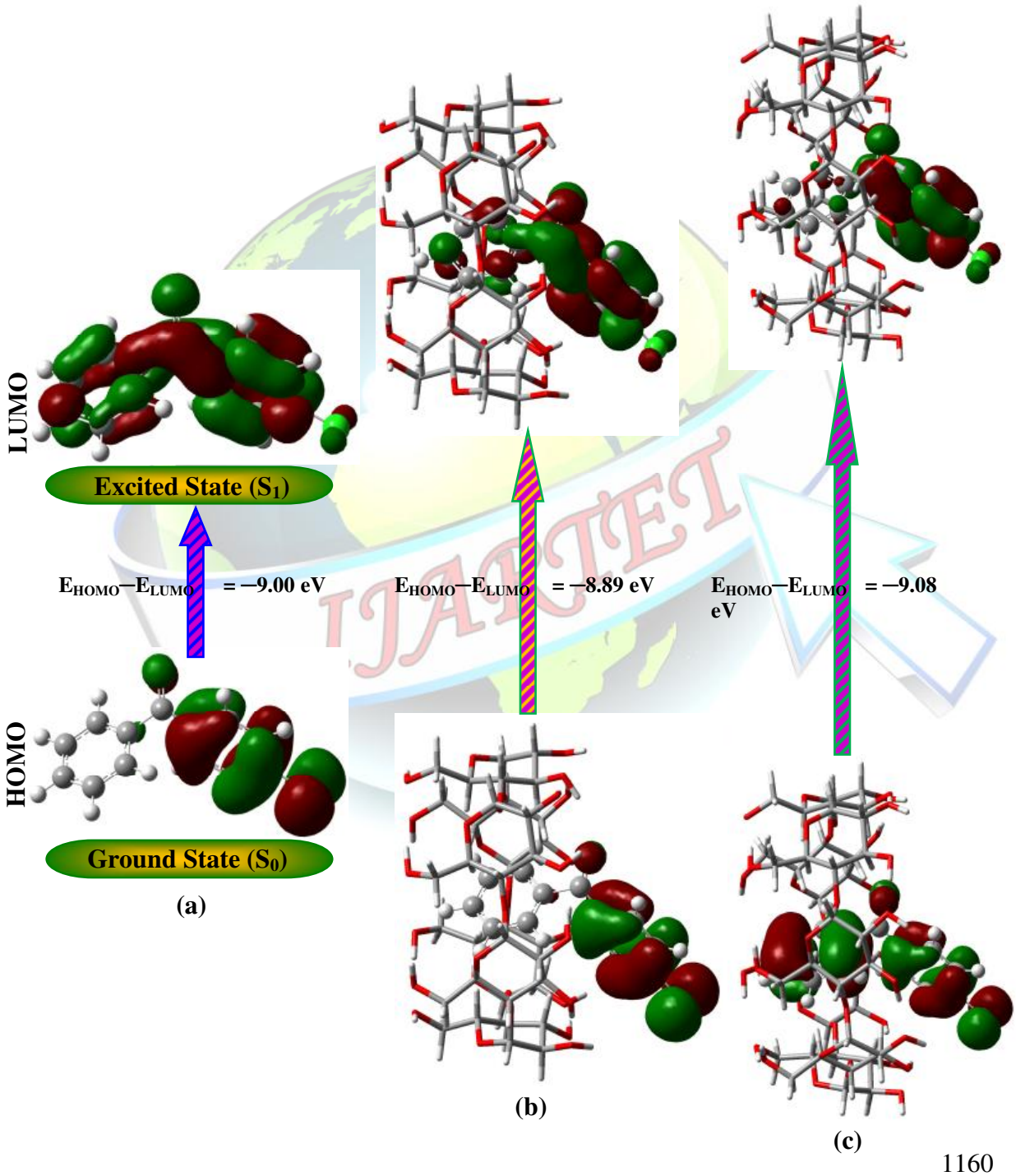

ISSN 2394-3777 (Print)
ISSN 2394-3785 (Online)
Available online at www.ijartet.com
International Journal of Advanced Research Trends in Engineering and Technology (IJARTET)
Vol. 3, Special Issue 2, March 2016

Fig. 7. The atomic orbital compositions of the frontier molecular orbital for (a) CBP, (b) CBP/α-CD (orientation-A) and (c) CBP/β-CD complex (orientation-A).

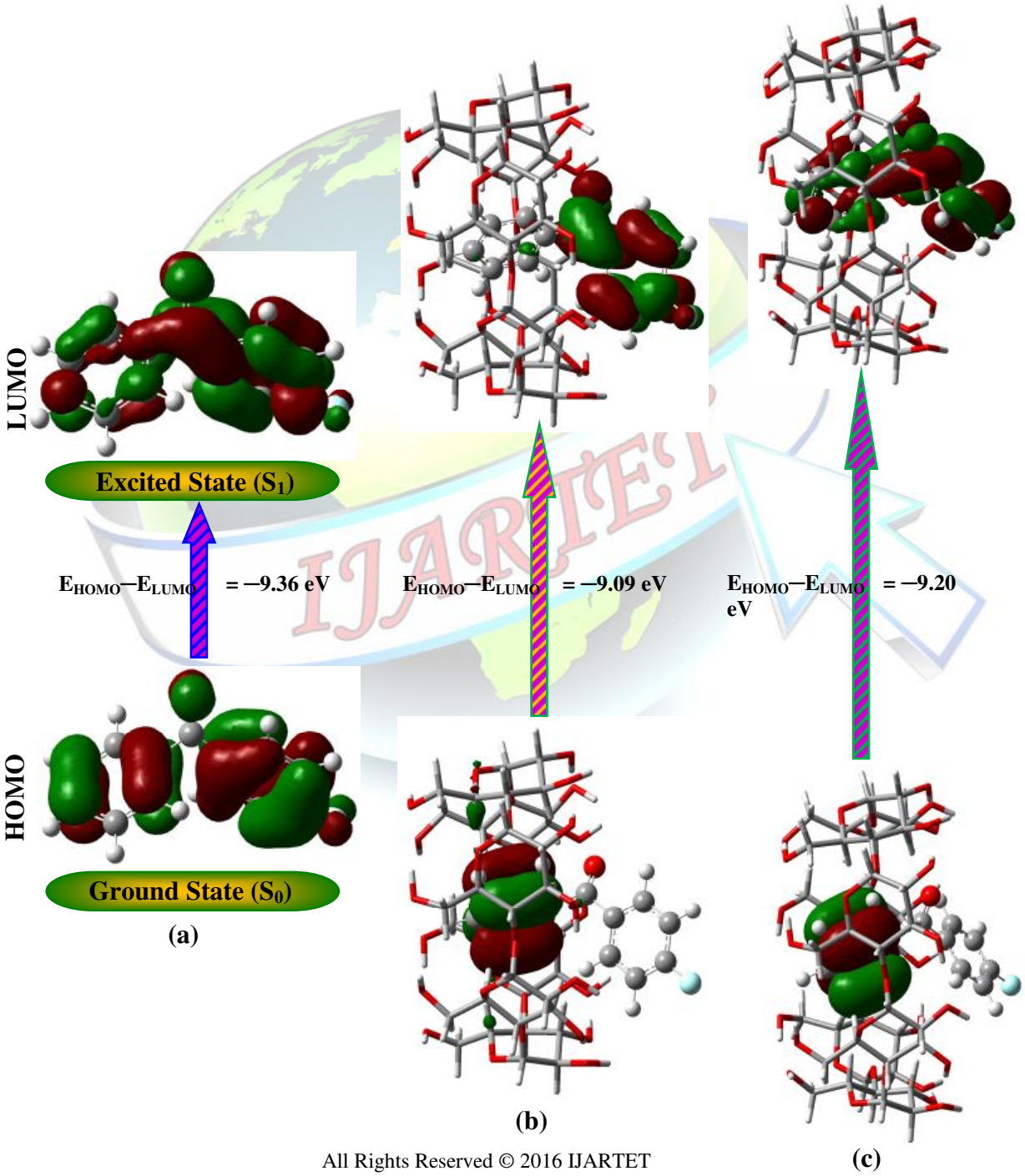

ISSN 2394-3777 (Print)
ISSN 2394-3785 (Online)
Available online at www.ijartet.com
International Journal of Advanced Research Trends in Engineering and Technology (IJARTET)
Vol. 3, Special Issue 2, March 2016

Fig. 8. The atomic orbital compositions of the frontier molecular orbital for (a) FBP, (b) FBP/α-CD (orientation-A) and (c) FBP/β-CD complex (orientation-A).

CHAPTER IV
SUMMARY

The present study reported a theoretical analysis in gas phase for the inclusion processes of three halogenated benzophenones (BBP, CBP and FBP) with α-CD and β-CD. Semiempirical PM3 method were used to calculate geometries and stabilization energies for all species, including free guests (BPs), hosts (α-CD and β-CD) and their respective inclusion complexes. The main conclusions drawn from the overall results can be summarized as follows: (i) The inclusion complex with β-CD (BPs/β-CD) is found to be more stable than the corresponding complex with α-CD (BPs/α-CD); (ii) The intermolecular hydrogen bonds established between the guest and host play a primary role to the complex stability. (iii) β-CD shows better ability to accommodate BPs and form (BPs/β-CD) inclusion complex with 1:1 stoichiometry. (iv) The negative enthalpy change (ΔH) suggested that all the inclusion processes were exothermic. The statistical thermodynamic calculations suggested that these inclusion complex processes are enthalpically favourable in nature. Finally, the present analysis suggests that the right choice of host molecule can be used to control the complex stability and therefore, might be used as guide in designing novel medicines based on inclusion compounds with different releasing time.

REFERENCES

[1] P. Rodríguez, M. Sánchez, J.R. Isasi, G. González-Gaitano, Appl. Spectrosc. 56 (2002) 1490.
[2] A. Kokkinou, S. Makedonopoulou, D. Mentzafos, Carbohydr. Res. 328 (2000) 135.
[3] M. Filippa, M.I. Sancho, E.J. Gasull, Pharm. Biomed. Anal. 48 (2008) 969.
[4] C. Cannava, V. Crupi, P. Ficarra, M. Guardo, D. Majolino, A. Mazzaglia, R. Stancanelli, V.J. Venuti, Pharm. Biomed. Anal. 51 (2010) 1064.
[5] M. Cirri, F. Maestrelli, N. Mennini, P.J. Mura, Pharm. Biomed. Anal. 50 (2009) 690.
[6] J.W. Steed, J.L. Atwood, Supramolecular Chemistry, Wiley-VCH, Weinheim, 2000.
[7] K. Martina, D.S. Puntambekar, A. Barge, M. Gallarate, D. Chirio, G. Cravotto, Carbohydr. Res. 345 (2010) 191.
[8] K. Uekama, F. Hirayama, T. Irie, Chem. Rev. 98 (1998) 2045.
[9] H.K. Fromming, J. Szejtli, Cyclodextrins in Pharmacy, Kluwer Academic Publishers, Dordrecht (1994).
[10] J. Szejtli, Chem. Rev. 98 (1998) 1743.
[11] L. Liu, Q.X. Guo, *J. Incl. Phenom. Macrocycl. Chem.* 50 (2004) 95.
[12] Y.J. Zheng, S.M. Legrand, M.K. Merz Jr., *J. Comput. Chem.* 13 (1992) 1151.
[13] C. Yan, Z. Xiu, X. Li, H. Teng, C. Hao, *J. Incl. Phenom. Macrocyclic Chem.* 58 (2007) 337.
[14] X. Li, L. Liu, T.W. Mu, Q.-X. Guo, *Monatsh. Chem.* 131 (2000) 849.
[15] T. Steiner, G. Koellner, *J. Am. Chem. Soc.*, 116 (1994) 5122.
[16]. S. Chaudhuri, S. Chakraborty, P.K. Sengupta, *J. Mol. Struct.*, 975 (2010) 160.
[17] E. Engeldinger, D. Armspach, D. Matt, P. G. Jones, R. Welter, *Angew. Chem., Int. Ed.* 41 (2002) 2593.
[18] E. Engeldinger, D. Armspach, D. Matt, P. G. Jones, *Chem. Eur. J.* 9 (2003) 3091.
[19] E. Engeldinger, D. Armspach, D. Matt, *Chem. Rev.* 103 (2003) 4147.
[20] M. I. Sancho, E. Gasull, S. E. Blanco, E. A. Castro, *Carbohyd. Res.* xxx (2011) xxx–xxx .
[21] K. Linderner, W. Saenger, *Carbohyd. Res.*, 99 (1982) 103.
[22] S. Holt Jennifer, *J. Mol. Struc.*, 965 (2010) 31.
[23]. C.L. Yan, Z.L. Xiu, X.H. Li, C. Hao, *J. Mol. Graph. Model.*, 26 (2007) 420.
[24] N. Rajendiran, S. Siva, Carbohydr. Polym. 101 (2014) 828–836.

ISSN 2394-3777 (Print)
ISSN 2394-3785 (Online)
Available online at www.ijartet.com
International Journal of Advanced Research Trends in Engineering and Technology (IJARTET)
Vol. 3, Special Issue 2, March 2016

[25] N. Rajendiran, S. Siva, J. Saravanan, J. Mol. Struct. 1054-1055 (2013) 215.
[26] E. Junquera, F. Mendicuti, E. Aicart, *Langmuir,* 15 (1999) 4472.
[27] M. Karelson, V.S. Lobanov, R. Katrizky, *Chem. Rev.*, 96 (1996) 1027.